THE JOURNAL OF COMPARATIVE NEUROLOGY 449:180–194 (2002)

Functional Mapping of the Rat Olfactory Bulb Using Diverse Odorants Reveals Modular Responses to Functional Groups and Hydrocarbon Structural Features

BRETT A. JOHNSON,* SABRINA L. HO, ZHE XU, JOANNE S. YIHAN, SALLIS YIP, EDNA E. HINGCO, AND MICHAEL LEON
Department of Neurobiology and Behavior, University of California, Irvine, California 92697-4550

ABSTRACT

In an effort to understand the olfactory code of rats, we collected more than 1,500,000 measurements of glomerular activity in response to 54 odorants selected to provide differences in functional groups and hydrocarbon structure. Each odorant evoked a unique response pattern by differentially stimulating clusters of glomeruli, called modules. Odorants sharing specific aspects of their structure activated the same modules, allowing us to relate responses to structure across approximately 80% of the glomerular layer. The most obvious relationship was between the presence of particular oxygen-containing functional groups and the activity of glomeruli within dorsal modules. Functional group-specific responses were observed for odorants possessing a wide range of hydrocarbon structure, including aliphatic, cyclic, and aromatic features. Even formic acid and acetone, the simplest odorants possessing acid or ketone functional groups, respectively, stimulated modules specific for these functional groups. At the same time, quantitative analysis of pattern similarities revealed relationships in activation patterns between odorants of similar hydrocarbon structure. The odorant responses were reliable enough to allow us to predict accurately specific aspects of odorant molecular structure from the evoked glomerular activity pattern, as well as predicting the location of glomerular activity evoked by novel odorants. J. Comp. Neurol. 449: 180–194, 2002.

Indexing terms: deoxyglucose; imaging; mapping; odor; sensory coding

A code is a set of rules by which information is transformed from one form into another. In the case of the neural coding of olfactory stimuli, the original information is in the form of volatile chemicals. By virtue of selective interactions with odorant receptors, molecular features of odorant molecules stimulate olfactory sensory neurons (Malnic et al., 1999), which directly innervate glomeruli of the olfactory bulb within the brain. Axons from sensory neurons expressing the same odorant receptor gene converge into a very few, stereotypically located glomeruli, suggesting that the spatial pattern of activated glomeruli may contain a representation of the molecular features present in odorants (Ressler et al., 1994; Vassar et al., 1994). Thus, part of the neural code responsible for odor perception may involve a spatially specific activity pattern in the bulb. If such a code exists, one should be able to predict the pattern of activity from the chemical structure of the odorant. As importantly, one should be able to identify the odorant from the spatial activity pattern.

To explore the possibility of spatial coding in the olfactory bulb, researchers have exposed rats to odorants dif-

Grant sponsor: NIDCD; Grant number: DC03545.

*Correspondence to: Brett A. Johnson, Department of Neurobiology and Behavior, University of California, 2205 McGaugh Hall, Irvine, CA 92697-4550. E-mail: bajohnso@uci.edu

Received 18 December 2001; Revised 13 April 2002; Accepted 13 April 2002

DOI 10.1002/cne.10284

Published online the week of June 10, 2002 in Wiley InterScience (www.interscience.wiley.com).

fering incrementally in chemical structure and have characterized differences in the spatial patterns of glomerular activity (Johnson et al., 1998, 1999; Rubin and Katz, 1999, 2001; Johnson and Leon, 2000a,b; Uchida et al., 2000; Meister and Bonhoeffer, 2001; Wachowiak and Cohen, 2001). Many of the odorants studied to date differ only slightly in carbon number, hydrocarbon branch structure, or functional group. Despite these small differences in chemical structure, the odorants evoke reliably different activity patterns. The patterns are composed of sets of glomerular modules, which are clusters of glomeruli that have similar specificity (Johnson et al., 1998, 1999; Johnson and Leon, 2000a,b). Pairs of chemically similar odorants tend to overlap in their activation of particular glomeruli and glomerular modules, such that the uniqueness of a given odorant is apparent only by considering the entire combination of glomeruli or modules activated (Johnson et al., 1998, 1999; Johnson and Leon, 2000a,b).

To decode any information contained within the spatial activity pattern, it will be necessary to determine the odorant characteristics responsible for activating particular modules. We found previously that odorants differing in oxygen-containing functional groups evoked activity in distinct modules, suggesting that these functional groups may be important molecular features represented by modules (Johnson and Leon, 2000a). Within certain modules, responses are arranged in space according to some molecular property of the odorant. For example, within a dorsal module responding to carboxylic acids and aldehydes, straight-chained molecules of incrementally greater carbon number stimulate increasingly rostral glomeruli (Johnson et al., 1999; Rubin and Katz, 1999; Uchida et al., 2000; Meister and Bonhoeffer, 2001). A similar arrangement is present within a module in the medial aspect of the bulb, where increasing carbon number shifts responses ventrally (Johnson et al., 1999). This arrangement reflects a preference of ventral glomeruli for odorants of greater molecular length rather than of greater volume or hydrophobicity, molecular aspects that co-vary with carbon number (Johnson and Leon, 2000b).

In addition to distinguishing odorants that differ only slightly in chemical structure, the olfactory system also detects odorants with very different structures, and any complete model of odor coding also must account for this capability. To explore more fully the range of odorant sensitivity in the rat olfactory system, we now have exposed rats to additional odorants that include aromatic, cyclic, and polycyclic structures, as well as a few additional molecules containing acyclic aliphatic structures. In a previous study, we found that odorants sharing a four-carbon, straight-chained hydrocarbon structure, but differing in the oxygen-containing functional group at the fifth position, differed in their activation of certain dorsal glomerular modules (Johnson and Leon, 2000a). To determine whether responses of these dorsal modules could be attributed primarily to odorant functional groups, we compared the activity patterns of other odorants possessing the same functional groups, but with very different hydrocarbon structures. Similarly, we determined whether activity in other glomerular modules predicts the presence of molecular features other than oxygen-containing functional groups.

MATERIALS AND METHODS

Odorant exposures

Sources of odorants and conditions for exposures are summarized in Table 1. In a typical experiment, young male Wistar rats (postnatal day [P] 18–22) from the same litter were exposed either to odorants of similar chemistry or to the appropriate vehicle. (The University of California, Irvine Institutional Animal Care and Use Committee approved all procedures involving rats.) For odorant sets including solid compounds, all related odorants first were dissolved in a solvent (mineral oil or ethanol). In such a case, the solvent served as the vehicle blank. In experiments involving only liquid odorants, all odorants were used neat, and air served as the vehicle blank. Odorants were volatilized by bubbling high-purity nitrogen gas (or air for ethyl acetate, ethyl butyrate, isoamyl acetate, and isoamyl butyrate) through a column of liquid in a gas-washing bottle. For neat odorants or odorants dissolved in ethanol, either 100 ml of odorant were used in a 125-ml washing bottle or 200 ml of odorant were used in a 250-ml washing bottle. For odorants dissolved in mineral oil, 200 ml of odorant were used in a 500-ml washing bottle. Volatilized odorants then were diluted further by mixing the vapor with a stream of ultra-zero grade air and were presented at a final flow rate of 2 L/min. Flow rates of odorant vapor were regulated and measured by using Gilmont flow meters. Components of the exposure apparatus in contact with odorant vapor were composed of glass, Teflon, Kynar, or brass, substances chosen for their low reactivity and low tendency to bind odorants.

In past studies, care was taken to equalize vapor phase concentrations of odorants within any given experiment (Johnson et al., 1998; 1999; Johnson and Leon, 2000a,b.). This level of equality was accomplished by estimating the vapor pressure from chemical class and boiling point by using an equation designed for molecules possessing single functional groups and simple hydrocarbon structures (Hass and Newton, 1975). Where possible, we have used this equation for the new odorants used in the present study (Table 1). Many of the new odorants, however, are complex hydrocarbons, some of which possess multiple functional groups (Fig. 1B) and some of which were dissolved in solvents that would alter the relationship between boiling point, chemical class, and vapor pressure (Segel, 1975). As such, their final concentrations are not likely to be estimated well by using this equation. Furthermore, published values for the vapor pressure of any individual molecule can vary widely. Because of these difficulties in equalizing vapor phase concentrations, we have opted instead to present most odorants at the highest concentration obtainable with our standard exposure protocol. High odorant concentrations increase the likelihood that strong patterns of 2-DG uptake will be available for analysis.

For several odorants (propanol, propionic acid, α-ionone, limonene, α-phellandrene, menthol, menthone, menthyl acetate, and menthyl isovalerate), we also exposed animals to at least one lower concentration. For all of these odorants, the pattern of activity evoked by the lower concentration was indistinguishable from the pattern evoked by the higher concentration. The lack of a change in pattern with odorant concentration is the same result that we have reported previously for caproic acid, valeric acid,

TABLE 1. Conditions for Odorant Exposures[1]

Odorant	Formula	Vendor	Purity (%)	Solvent	Dilution in Solvent	Dilution in Air	ppm in Vapor Phase	n	Reference
Formic acid	CH_2O_2	Fisher	n.r.	Water	0.85	0.0024	100	6	F
Acetic acid	$C_2H_4O_2$	Fisher	99.7	None	None	0.00045	7.2	6	A
Propionic acid	$C_3H_6O_2$	Fisher	>99	None	None	0.0017	7.2	6	A
Butyric acid	$C_4H_8O_2$	Fisher	99	None	None	0.0096	7.2	6	A
Valeric acid	$C_5H_{10}O_2$	Fisher	99	None	None	0.125	25	3	F
Caproic acid	$C_6H_{12}O_2$	Fisher	98	None	None	0.052	4	6	B
Octanoic acid	$C_8H_{16}O_2$	Fisher	>99.5	None	None	0.111	0.8	6	A
Isovaleric acid	$C_5H_{10}O_2$	Fisher	99	None	None	0.026	8	6	B
2-Methylbutyric acid	$C_5H_{10}O_2$	Fisher	98	None	None	0.026	8	6	B
Isocaproic acid	$C_6H_{12}O_2$	Fisher	99	None	None	0.046	4	6	B
tert-Butylacetic acid	$C_6H_{12}O_2$	Fisher	98	None	None	0.021	4	6	B
Cyclobutanecarboxylic acid	$C_5H_8O_2$	Fisher	98	None	None	0.081	8	6	B
Cyclopentanecarboxylic acid	$C_6H_{10}O_2$	Fisher	98	None	None	0.126	4	6	B
trans-2-Pentenoic acid	$C_5H_8O_2$	Fisher	97	None	None	0.125	8	6	B
trans-3-Hexenoic acid	$C_6H_{10}O_2$	Fisher	99	None	None	0.076	4	6	B
Methanol	CH_4O	Fisher	99.9	None	None	0.018	2500	6	F
Pentanol	$C_5H_{12}O$	Fisher	99	None	None	0.094	250	3	C
Acetone	C_3H_6O	Fisher	99.5	None	None	0.0093	2500	6	F
2-Hexanone	$C_6H_{12}O$	Fisher	98	None	None	0.016	250	3	C
Pentanal	$C_5H_{10}O$	Fisher	98	None	None	0.0071	250	3	C
Ethyl acetate	$C_4H_8O_2$	Fisher	>99.5	None	None	0.00061	750	3	D
Ethyl butyrate	$C_6H_{12}O_2$	Fisher	99	None	None	0.004	750	3	D
Methyl valerate	$C_6H_{12}O_2$	Fisher	99	None	None	0.019	250	3	C
Isoamyl acetate	$C_7H_{14}O_2$	Sigma	98	None	None	0.011	750	3	D
Isoamyl butyrate	$C_9H_{18}O_2$	Fisher	>99	None	None	0.071	750	3	D
(+)- and (−)-Limonene	$C_{10}H_{16}$	Aldrich	97,95	None	None	0.125	n.d.	6	E
(+)- and (−)Carvone	$C_{10}H_{14}O$	Fisher	98	None	None	0.125	n.d.	6	E
(+)- and (−)-Terpinen-4-ol	$C_{10}H_{18}O$	Fisher	95,97	None	None	0.125	n.d.	6	E
Propanol	C_3H_8O	Fisher	>99	None	None	0.10	2500	3	F
Hexanol	$C_6H_{14}O$	Fisher	98	None	None	0.0091	7.2	6	F
Octanol	$C_8H_{18}O$	Fisher	>99	None	None	0.085	7.2	6	F
Geraniol	$C_{10}H_{18}O$	Fisher	99	None	None	0.125	n.d.	3	F
Santalol	$C_{15}H_{24}O$	Aldrich	96	None	None	0.125	n.d.	3	F
Decanal	$C_{10}H_{20}O$	Fisher	95	None	None	0.125	n.d.	3	F
Benzaldehyde	C_7H_6O	Fisher	>98	Ethanol	0.1	0.125	n.d.	6	F
o-, *p*-, and *m*-Anisaldehyde	$C_8H_8O_2$	Fisher	97–98	Ethanol	0.1	0.125	n.d.	6	F
Vanillin	$C_8H_8O_3$	Fisher	99	Ethanol	0.1	0.125	n.d.	3	F
4-Hydroxybenzaldehyde	$C_7H_6O_2$	Fisher	99	Ethanol	0.1	0.125	n.d.	3	F
Guaiacol	$C_7H_8O_2$	Fisher	>99	Ethanol	0.1	0.125	n.d.	3	F
α-Phellandrene	$C_{10}H_{16}$	Aldrich	n.r.	Mineral oil	0.25	0.05	n.d.	6	F
L-Menthol	$C_{10}H_{20}O$	Aldrich	>99	Mineral oil	0.25	0.05	n.d.	6	F
L-Menthone	$C_{10}H_{18}O$	Aldrich	>96	Mineral oil	0.25	0.05	n.d.	6	F
Menthyl acetate	$C_{12}H_{22}O_2$	Aldrich	>97	Mineral oil	0.25	0.05	n.d.	6	F
Menthyl isovalerate	$C_{15}H_{28}O_2$	Aldrich	>98	Mineral oil	0.25	0.05	n.d.	6	F
α-Ionone	$C_{13}H_{20}O$	Aldrich	>90	None	None	0.125	n.d.	3	F
D-Camphor	$C_{10}H_{16}O$	Fisher	97	Mineral oil	0.025	0.05	n.d.	3	F
β-Pinene	$C_{10}H_{16}$	Fisher	98	Mineral oil	0.025	0.05	n.d.	3	F
Naphthalene	$C_{10}H_8$	Fisher	99	Mineral oil	0.0062	0.05	n.d.	3	F
2-Acetylpyridine	C_7H_7NO	Fisher	98	None	None	0.125	n.d.	3	F

[1]Where possible, vapor phase concentrations were estimated using the equation of Hass and Newton (1975) and are displayed as parts per million (ppm). n.r., not reported by supplier; n, number of rats studied; n.d., not determined. References to previous studies are as follows: A, Johnson et al., 1999; B, Johnson and Leon, 2000b; C, Johnson and Leon, 2000a; D, Johnson et al., 1998 (remapped by using the current method); E, Linster et al., 2001; F, present study.

methyl valerate, and pentanol (Johnson et al., 1999; Johnson and Leon, 2000a). Nevertheless, low and high concentrations of pentanal and 2-hexanone, which evoke distinct odor perceptions in humans, evoked different patterns of activity in our previous study (Johnson and Leon, 2000a). Therefore, it remains possible that for some of the odorants in the present study, the pattern could have been different had we used some other concentration. On several occasions, we exposed distinct sets of rats to the same odorant at the same concentration. There was little variation in the evoked pattern across the different experiments. Patterns arising both from exposures to different concentrations of odorants and from different experiments using the same odorants and concentrations can be viewed at our Web site (http://leonlab.bio.uci.edu).

2-Deoxyglucose method

As our measure of glomerular activity, we used uptake of [^{14}C]-2-deoxyglucose (2-DG), which can quantify responses throughout the entire olfactory bulb (Stewart et al., 1979; Jourdan et al., 1980; Royet et al., 1987; Johnson et al., 1999), an aspect of our analysis that was essential for the correct interpretation of our results. Immediately before odorant exposure, rats were injected subcutaneously with 0.16–0.2 mCi/kg [^{14}C]2-DG (Sigma Chemical Company, St. Louis, MO). The awake, naturally respiring rats then were exposed to the odorant for 45 minutes in a mason jar by using our standard techniques (Johnson et al., 1999). The 2-DG technique does not investigate the temporal parameters of the neural response, but rather quantifies relative neural activity with a spatial resolution allowing the detection of individual active glomeruli (Johnson et al., 1998; Linster et al., 2001).

Mapping procedure

Fresh-frozen brains were sectioned at a thickness of 20 μm by using a cryostat. Every sixth section was exposed to autoradiography film, and adjacent sections were stained with cresyl violet to identify both the glomerular layer and the anatomic landmarks that are used to standardize

maps along the rostral–caudal dimension (Johnson et al., 1999). Uptake was sampled at discrete locations guided by polar grids as described previously (Johnson et al., 1999). Measurements (approximately 2,500 per bulb) were incorporated into anatomically standardized data arrays and transformed into units of tissue equivalents of radioactivity by comparison with standards. Arrays for left and right bulbs of the same animal were averaged and then transformed into units of glomerular layer uptake/subependymal zone uptake (Johnson et al., 1999). Similarly transformed arrays from animals exposed to the appropriate vehicle (air, mineral oil, or ethanol) were averaged and subtracted from arrays for each odorant-exposed animal (Johnson and Leon, 2000a). Values within an array then were converted into units of z scores relative to the mean and standard deviation of values calculated across that array (Johnson et al., 1999). The resulting z-score arrays were averaged across the different animals exposed to the same odorant condition. The number of animals averaged for each odorant is shown in Table 1.

Quantitative comparisons of odorant-evoked patterns

To get an objective measure of the degree of similarity between average z-score activity patterns evoked by different odorants, we calculated Pearson correlation coefficients for odorant pairs. In these calculations, X-Y pairs represented corresponding individual cells in the data arrays, such that each coefficient generally involved approximately 2,500 X-Y pairs. Only odorant-evoked patterns from which vehicle blank patterns had been subtracted were used. By using a sample of over 20 odorants evoking a combination of very similar and very different pairs of patterns, we found that the Pearson coefficients were closely and inversely correlated with indices of pattern dissimilarity such as we had calculated in past studies (Johnson et al., 1999; Johnson and Leon, 2000a). In this comparison, a pattern dissimilarity index of 1.1 was found to correspond to a Pearson coefficient of 0 (no correlation).

Contour charts

Contour charts were produced by using Microsoft Excel 2001. The images then were exported as GIF files by using the "Save as Web Page" feature, followed by labeling in Canvas 7 (Deneba Systems, Inc., Miami, FL).

RESULTS

Odorants possessing the same functional groups activate the same glomerular modules

As shown in previous reports (Johnson et al., 1999; Johnson and Leon, 2000a,b), all 14 of the carboxylic acids we had studied previously (Fig. 1A) activated glomeruli in the anterior, dorsal part of the bulb, which we have labeled module "a" (Fig. 2). Every acid also activated a corresponding dorsomedial module "A." The responses to cyclobutanecarboxylic acid, tert-butylacetic acid, and octanoic acid are shown in Figure 2 (upper left), with modules "a" and "A" outlined in black. The activation of modules "a" and "A" by carboxylic acids of very different hydrocarbon structure argues for a generalized recognition of the acid functional group by these modules. If, as suggested by these data, modules "a" and "A" recognize the acid functional group independently of odorant hydrocarbon structure, then one would predict that the modules would respond to the simplest odorants containing this functional group. Therefore, we tested the response to formic acid, which possesses only one carbon. As shown in Figure 3, formic acid indeed stimulated modules "a" and "A", strongly suggesting that these modules respond primarily to the acid functional group.

We previously showed (Johnson and Leon, 2000a) that the ketone 2-hexanone activated a dorsal module (module "c") located more caudally than module "a," as well as a corresponding dorsomedial module "C" (Fig. 2, middle left), and we predicted that other ketones also would activate the same module. As shown in Figure 2, other odorants possessing the ketone functional group did stimulate modules "c" and "C," including odorants with both quite distinct hydrocarbon structures and perceived odors, such as the cyclic menthone (peppermint), the cyclic L-carvone (spearmint), and the aromatic 2-acetylpyridine (popcorn). Even acetone, the simplest odorant possessing a ketone functional group, stimulated modules "c" and "C" (Fig. 3). Seven of eight ketones we studied (Fig. 1) stimulated modules "c" and "C," the only exception being the polycyclic odorant, D-camphor, which instead stimulated glomeruli located somewhat more ventrally and caudally, similar to what was described previously by Stewart and colleagues (1979).

In a previous report (Johnson and Leon, 2000a), we showed that the carboxylic ester methyl valerate stimulated a somewhat more ventral cluster of glomeruli (module "e") located midway between the rostral pole of the bulb and the beginning of the accessory olfactory bulb, as well as the corresponding medial module "E" (Fig. 2, lower left). Therefore, we predicted that esters, even with very different hydrocarbon structure should activate this glomerular module. In fact, all seven esters we have tested (Fig. 1) stimulated these paired modules. Shown along with methyl valerate in Figure 2, from left to right, are the responses to the shorter aliphatic ester ethyl acetate (pineapple odor), the longer aliphatic ester isoamyl butyrate (banana odor), and the cyclic ester menthyl isovalerate (woody or violet odor).

The aldehyde pentanal and the alcohol pentanol both stimulated modules "b" and "B" (Fig. 2, right) in our previous report (Johnson and Leon, 2000a). We found that other alcohols and aldehydes also activated glomeruli within these modules, including odorants both with longer straight-chained hydrocarbon structures and with compact aromatic hydrocarbon structures (Fig. 2, right). Interestingly, odorants with similar hydrocarbon structures stimulated similar regions within modules "b" and "B" independently of the presence of the alcohol or aldehyde group. For example, decanal and octanol stimulated more ventral parts of the modules, whereas o-anisaldehyde (almond or hay-like odor) and guaiacol (smoky odor) activated glomeruli located at the dorsal extremes of the modules (Fig. 2, right). This arrangement of responses within modules "b" and "B" recalls the chemotopic organization with respect to odorant molecular length that we have reported for carboxylic acids within modules "a" and "A" (Johnson et al., 1999; Johnson and Leon, 2000b).

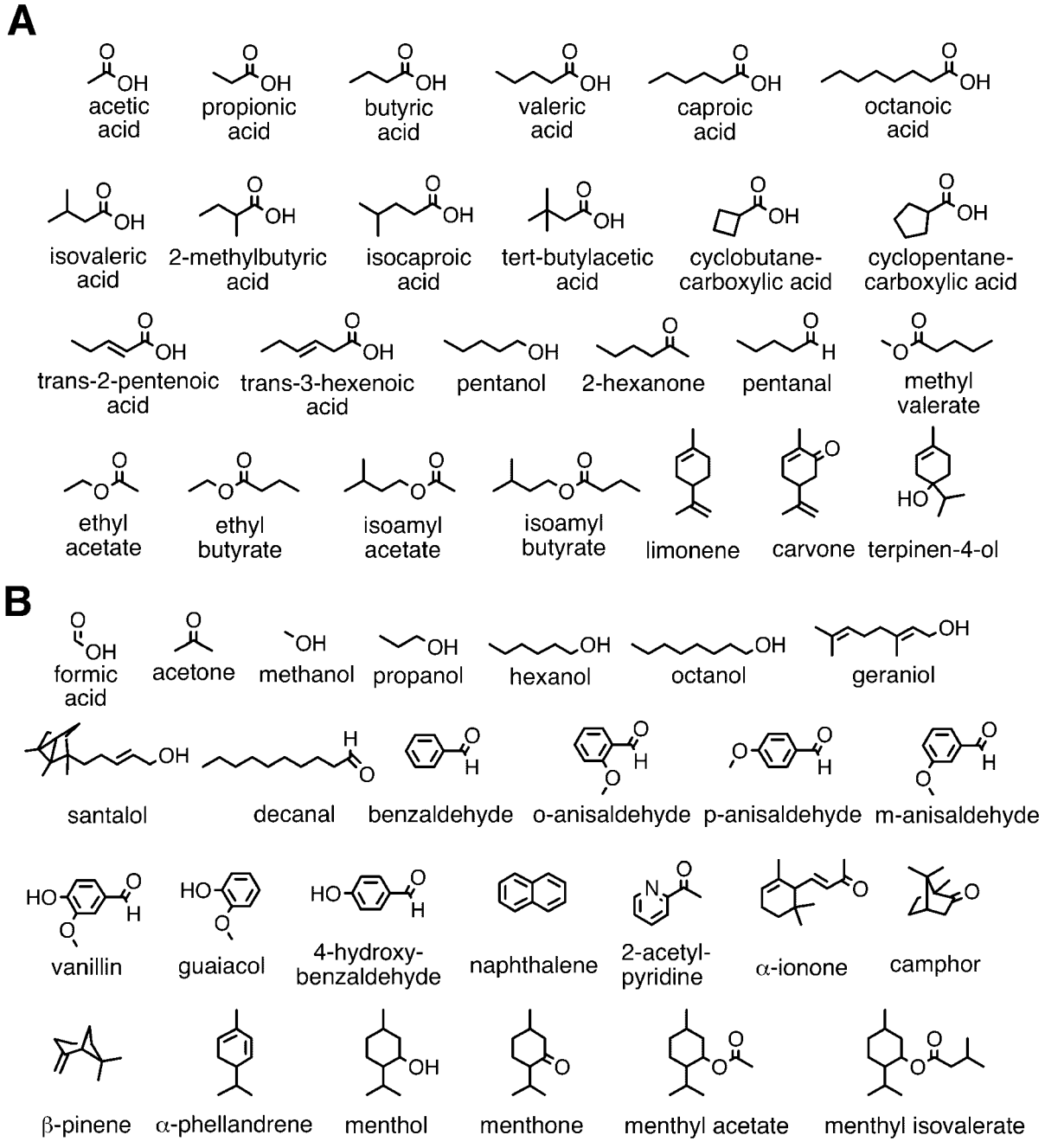

Fig. 1. Odorants investigated for evoked glomerular activity patterns. Lines indicate carbon bonds. Hydrocarbon hydrogens are omitted for clarity. **A:** Odorants used in previous studies. **B:** Odorants used in this study only.

Ventral modules respond to odorants with dense hydrocarbon features

As part of our investigation into odorant functional groups, we compared six odorants that occur together naturally in peppermint and that have similar hydrocarbon structures by virtue of being formed along the same metabolic pathway (Mann et al., 1993). Four of these compounds (menthol, menthone, menthyl acetate, and menthyl isovalerate) possessed oxygen-containing functional groups and evoked activity patterns involving modules activated by other compounds sharing those functional groups (Fig. 4, upper row). Two of the compounds, α-phellandrene and L-limonene (turpentine-like odors), do not have any oxygen-containing functional groups. In addition to strongly activating the midlateral and midmedial portions of the olfactory bulb,

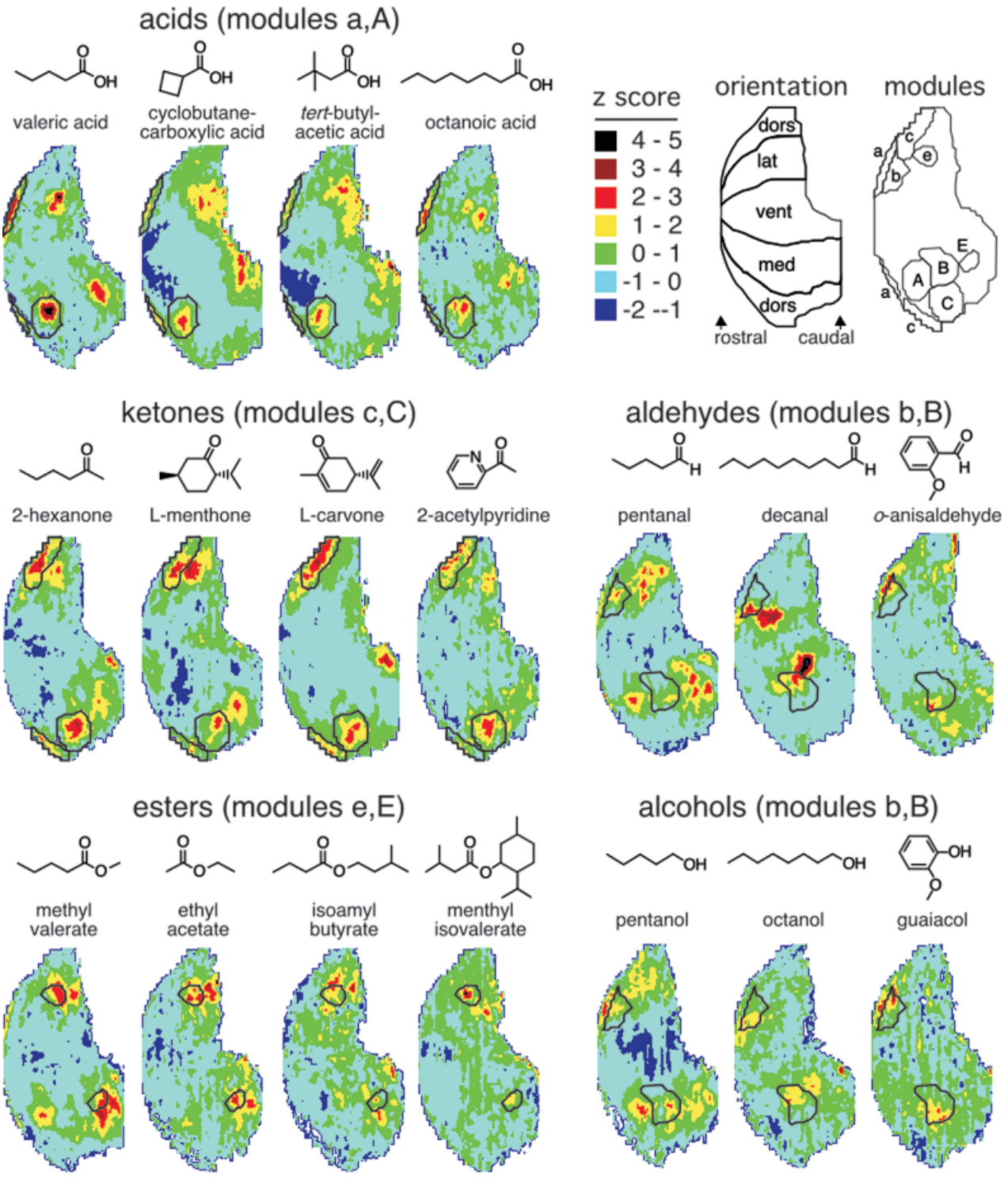

Fig. 2. Odorants sharing functional groups activate common glomerular modules. Contour charts indicate locations of 2-deoxyglucose uptake across the entire glomerular layer. Each chart shows activity averaged across both bulbs of numerous rats exposed to a given odorant. Relative uptake is color coded in units of z score according to the key at upper right. Also shown at upper right is the orientation of the contour charts with respect to olfactory bulb anatomy (dors, dorsal; lat, lateral; vent, ventral; med, medial), as well as an inset depicting the relative locations of modules identified in this work to respond specifically to functional groups. Within each panel, relevant modules indicated in the headers are outlined in black.

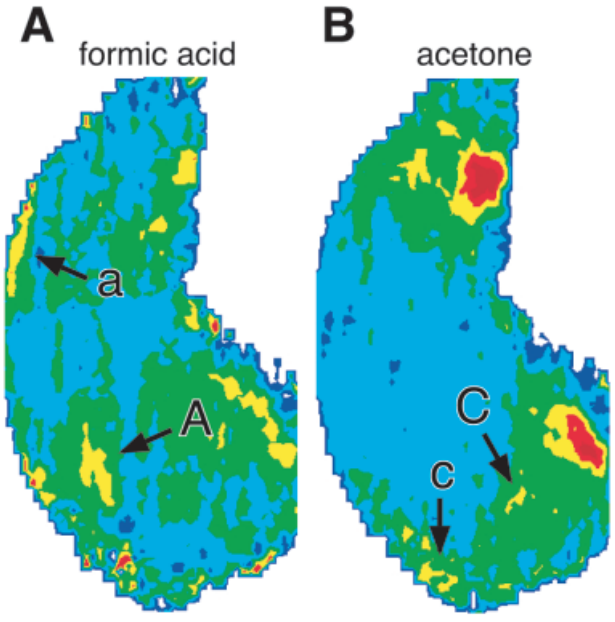

Fig. 3. Modular responses to the simplest odorants possessing acid (**A**) or ketone (**B**) functional groups. Note the activation of modules "a" and "A" by formic acid and the activation of modules "c" and "C" by acetone. Color-coding is as indicated in Figure 1.

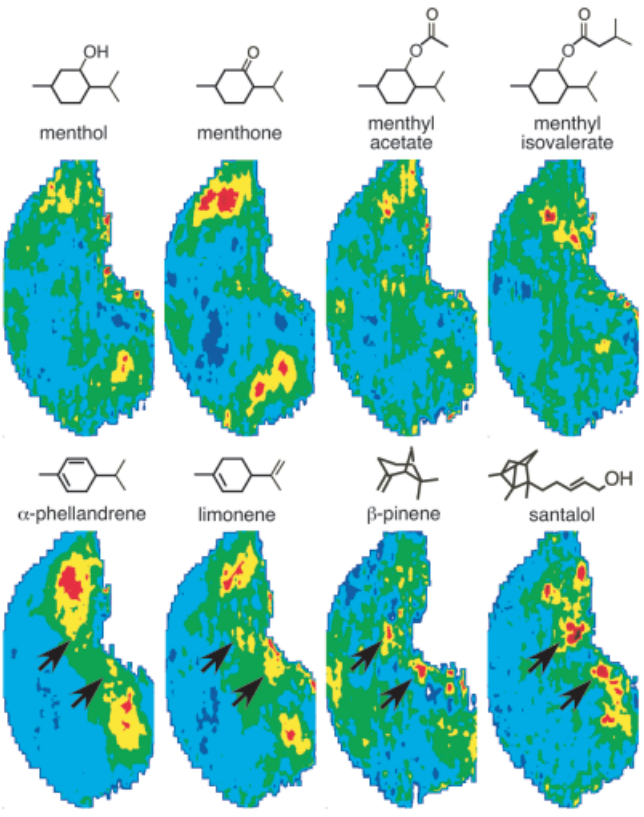

Fig. 4. Glomerular activity patterns for menthyl odorants and odorants with dense hydrocarbon features. Contour charts indicate the spatial distributions of 2-deoxyglucose uptake evoked by (top row, left to right) L-menthol, L-menthone, menthyl acetate, and menthyl isovalerate and by (bottom row, left to right) α-phellandrene, L-limonene, β-pinene, and santalol. Color-coding is as indicated in Figure 1. The two odorants related to menthol but lacking oxygen-containing functional groups, α-phellandrene and L-limonene, activated ventral regions not previously stimulated in our studies (arrows). These regions were activated even more strongly by β-pinene and by santalol, both of which have complex cyclic features characterized both by the presence of multiple hydrocarbon hydrogens in a small volume and by the absence of oxygen-containing functional groups.

these compounds stimulated glomeruli in regions more ventral than we had seen activated previously (Fig. 4, bottom left, arrows). Similar compounds without oxygen atoms have been found to activate sensory neurons in the ventral portions of the olfactory epithelium (Scott et al., 1996, 1997, 2000), which is in agreement with our bulbar pattern given the topography of the epithelium-to-bulb projection (Astic and Saucier, 1986; Schoenfeld et al., 1994).

Therefore, we predicted that a novel odorant sharing similar molecular features with α-phellandrene and L-limonene also would stimulate the posterior, ventral glomeruli. To test this prediction, we selected the odorant β-pinene (odor of pine), which also lacks oxygen-containing functional groups. This polycyclic odorant, which has many hydrocarbon hydrogens in a relatively small volume, activated the posterior, ventral glomeruli even more strongly than did α-phellandrene and L-limonene (Fig. 4, bottom row, third column, arrows). To determine whether a region of densely packed hydrocarbon hydrogens can be detected as a molecular feature in the context of an odorant that also possesses oxygen-containing functional groups, we exposed a group of rats to santalol (odor of sandalwood). Santalol has a polycyclic domain separated from an alcohol group by an aliphatic spacer. Indeed, santalol very robustly activated posterior, ventral modules (Fig. 4, bottom right, arrows), in addition to stimulating modules in more dorsal bulbar regions. These data indicate that the glomerular responses are sufficiently reliable and systematic to be able to predict the place at which novel odorants will activate the glomerular layer.

Predictions about chemical structure from spatial activity patterns

To locate any other new modules and to redefine the boundaries of previously proposed modules (Johnson and Leon, 2000a) in light of the new data, we traced apparent modules within the activity patterns evoked by each of the 54 odorants in Figure 1, and we superimposed these tracings on one another to identify modules that were present across different odorants. Figure 5 illustrates our current model of the modular representations of these odorants. We identified 26 modules (13 pairs of lateral and medial modules), each of which was activated by more than 3 of the 54 odorants. Approximately 80% of the olfactory bulb surface is included in these modules, which is a large percentage, given that the olfactory system can distinguish the odors of many thousands of odorant chemicals. To illustrate how modules are used differentially in the representation of distinct odorants, we averaged the z

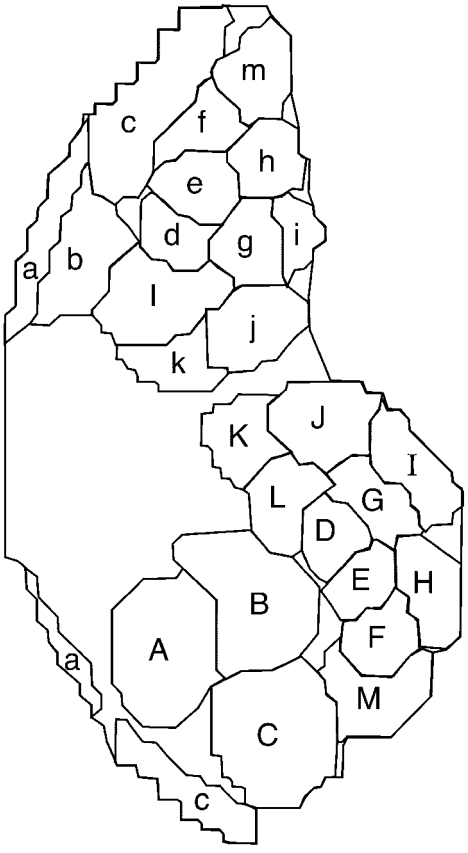

Fig. 5. Our current model of modular responses in the olfactory bulb. Apparent modular responses to odorants were outlined and superimposed on one another to identify modules used in the representations of multiple odorants. Shown here are those modules that were activated by more than three of the 54 odorants studied. For a great majority of the odorants, whenever a module was identified in the lateral aspect of the bulb, a module of similar activity was detected in the medial bulbar aspect. The corresponding lateral and medial modules are labeled here by using the same letter, lower case for the lateral representation and upper case for the medial representation.

score values within each module for each odorant. The results are shown in Figure 6, where the diameter of each circle indicates the relative magnitude of uptake for lateral (solid circles) and medial (hollow circles) modules (negative values are not shown).

Each odorant gave a unique pattern of modular activation, determined both by which modules were activated and by the relative amounts of uptake within the activated modules (Fig. 6). The differential activation of a limited set of modules attests to the combinatorial nature of the representation and is one reason why so many odorants can be represented uniquely by so few modules. The actual patterns of activity were even more distinct than depicted in Figure 6, which does not show the relative locations of activity within modules (Johnson et al., 1999; Johnson and Leon, 2000b), and which sometimes obscures very focal, high activity within a module. For example, such highly focal responses distinguish (−)-carvone from (+)-carvone within module "I" (Linster et al., 2001).

The patterns of uptake across the lateral modules were recapitulated by the patterns across the corresponding medial modules, as evidenced by the similarity of sizes of the adjacent solid and hollow circles in Figure 6. Indeed, the uptake in homologous lateral and medial modules was significantly and highly correlated (linear regression, $r = 0.79$, $P < 0.001$). The presence of nearly identical patterns within the lateral and medial aspects of the bulb is predicted from the projection patterns of olfactory sensory neurons expressing the same odorant receptors (Ressler et al., 1994; Vassar et al., 1994; Mombaerts et al., 1996) and has been observed in every study where we have mapped activity throughout the entire glomerular layer (Johnson et al., 1998, 1999; Johnson and Leon, 2000a,b). The major violations of this symmetry involved modules "i" and "I," as was suggested in a previous study using many fewer odorants (Johnson and Leon, 2000a). The posterior, ventromedial location of module "I," as well as its broad odorant specificity, suggests that the unpaired activity within this module may reflect responses of glomeruli that receive their projections exclusively from the septal organ (Marshall and Maruniak, 1986; Giannetti et al., 1992; Ma et al., 2001).

Despite the unique pattern evoked by each individual odorant, there were remarkable similarities across odorants possessing the same oxygen-containing functional groups (Fig. 6). These similarities indicate that the patterns of activity contain information regarding the molecular structure of the odorant molecules.

As mentioned above, all carboxylic acids in our current sample of odorants stimulated modules "a" and "A" (Fig. 6), but this information is not sufficient to identify an odorant as an acid, because aldehydes, as well as some alcohols and esters, also activated these modules. However, if an odorant that stimulates modules "a" and "A" does not much stimulate either modules "b/B" or "c/C," then one can be more confident that the odorant is an acid (Fig. 6).

Similarly, most ketones stimulated modules "c/C," but certain alcohols and aldehydes also activated these modules (Fig. 6). However, if an odorant that activates modules "c/C" does not much stimulate either modules "a/A" or "b/B," then one can be confident that the odorant is a ketone (Fig. 6). Previous results, however, demonstrated that lower concentrations of the ketone 2-hexanone did not activate modules "c/C" (Johnson and Leon, 2000a), so that the absence of activity in these modules does not indicate that the odorant is not a ketone.

If an odorant stimulates modules "b" and "B," the odorant is likely to be either an aldehyde or an alcohol (Fig. 6). It should be pointed out, however, that not all alcohols stimulated modules "b/B," which suggests that only specific hydrocarbon structures are accommodated by this module. Odorants possessing a wide variety of functional groups activated modules "e" and "E," but if an odorant strongly activates these modules without stimulating modules "a/A," "b/B," or "c/C," then one can be confident that the odorant is either an ester or a hydrocarbon lacking oxygen-containing functional groups.

Quantitative comparisons of patterns across odorants

In an effort to discover other similarities in odorant-evoked activity patterns, we compared patterns quantita-

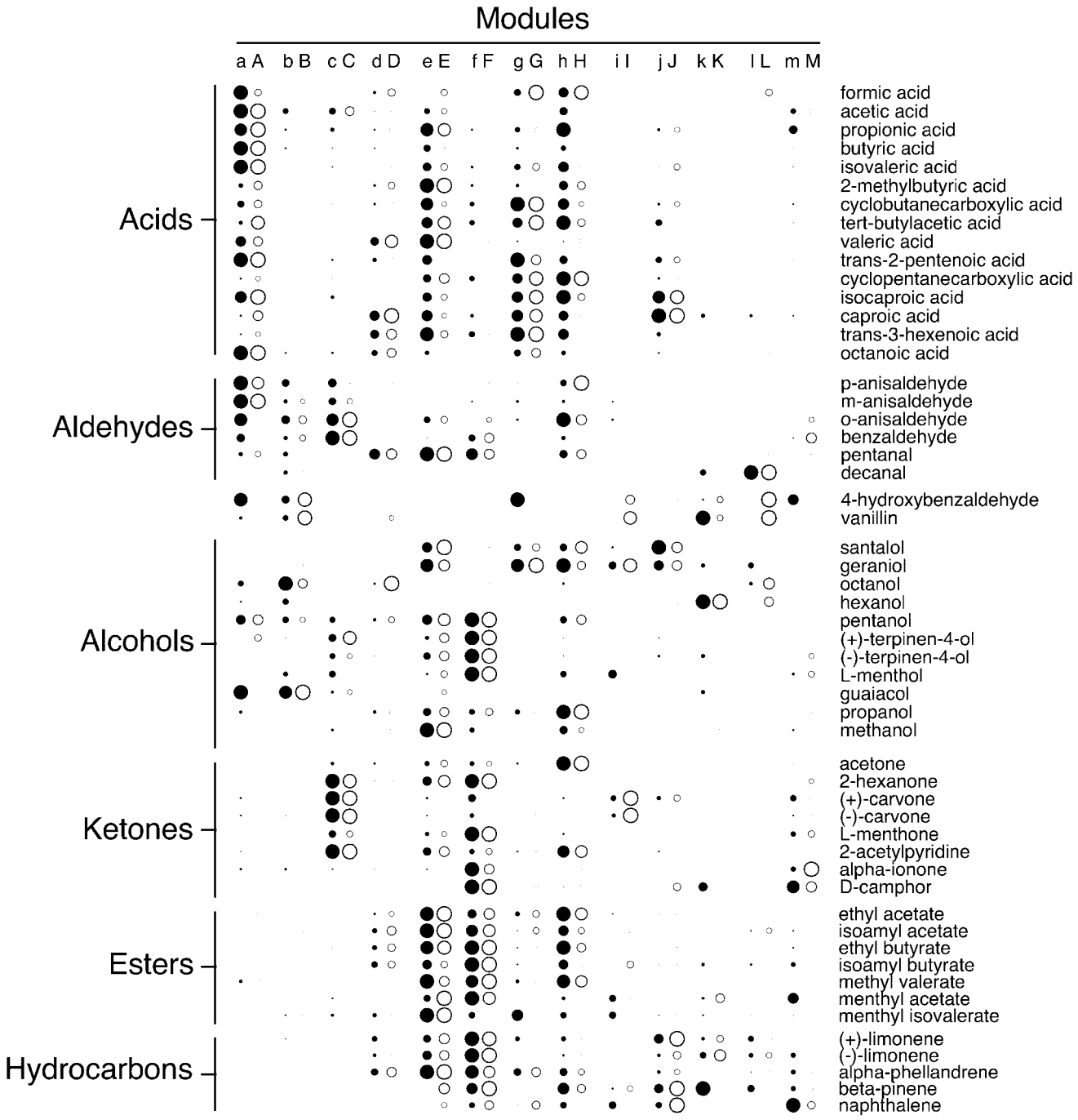

Fig. 6. Relative use of modules in the representations of individual odorants. For each odorant, z-score values were averaged across each of the glomerular modules shown in Figure 4. Each average was expressed as a fraction of the highest value of any module in the same aspect (lateral or medial), and these values then were symbolized by the diameters of circles. Solid circles are used for lateral modules, and hollow circles for medial modules. The odorants are subdivided according to functional groups as indicated at left. Two odorants, 4-hydroxybenzaldehyde and vanillin, have both aldehyde and alcohol functional groups.

tively by using an approach that does not bin data into glomerular modules. In this analysis, we determined Pearson correlation coefficients for pairs of activity patterns by using corresponding individual data points within the arrays as the source of X-Y pairs. To facilitate the visualization of the 946 coefficients resulting from all possible pairs of the 44 odorants in this analysis, the individual values are indicated by gray-scaled squares in the patchwork shown in Figure 7 (darker squares indicate greater pattern similarity). The top 25 correlations are further specified in Table 2.

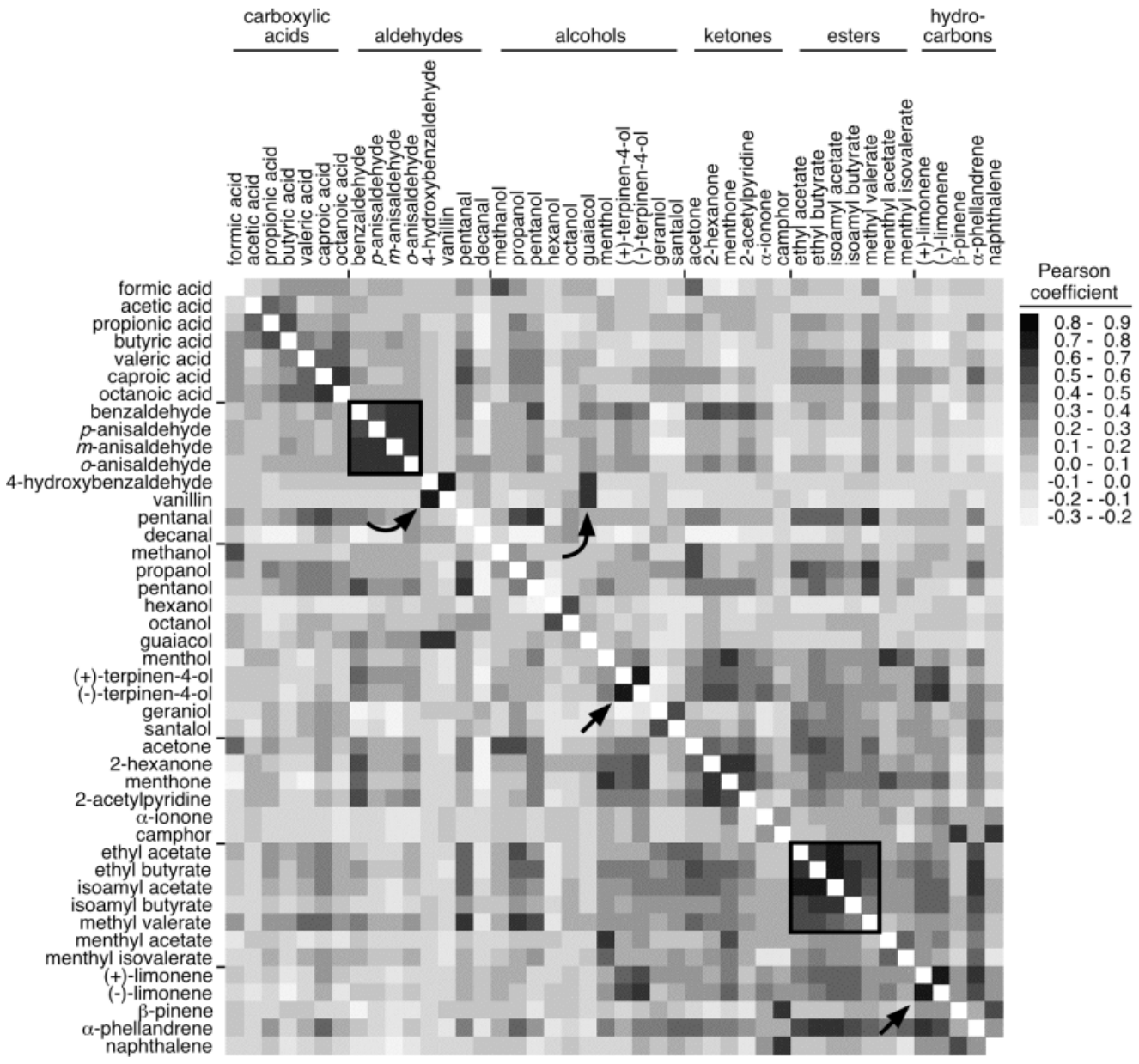

Fig. 7. Patchwork showing correlations between pairs of odorant-evoked glomerular activity patterns. Pearson correlation coefficients were used as an index of similarity between patterns. Coefficients were transformed into a gray scale code as shown on the right, with more similar patterns being indicated by darker squares. In general, the highest correlations were found for odorants having both the same functional groups and a similar hydrocarbon structure. Borders indicate two clusters of values indicating particularly high similarity, one involving five acyclic, aliphatic esters, the other involving positional isomers of anisaldehyde as well as benzaldehyde. Straight arrows indicate a high degree of similarity between enantiomers of limonene and terpinen-4-ol. Curved arrows indicate the similarities between vanillin, 4-hydroxybenzaldehyde, and guaiacol, which share a benzene ring and an alcohol functional group. As discussed in the text, many individual odorants also were found to be similar to other odorants possessing similar hydrocarbon structures but different functional groups.

This analysis showed that the greatest similarities in patterns involved odorants that were similar in both functional group and hydrocarbon structure. For example, particularly high correlations were obtained between the various aliphatic, acyclic esters (black borders in Fig. 7, lower right), between enantiomer pairs of limonene and terpinen-4-ol (straight arrows in Fig. 7), and between positional isomers of anisaldehyde as well as benzaldehyde (black borders in Fig. 7, upper left). Other such examples were 4-hydroxybenzaldehyde, vanillin, and guaiacol, odorants that share both a benzene ring and an alcohol functional group, although

TABLE 2. Most Similar Odorant-Evoked Activity Patterns

		Comparison	
Rank	r	Odorant 1	Odorant 2
1	0.777	Ethyl acetate	Isoamyl acetate
2	0.758	Ethyl butyrate	Isoamyl acetate
3	0.745	(+)-terpinen-4-ol	(−)-terpinen-4-ol
4	0.740	(+)-limonene	(−)-limonene
5	0.717	4-hydroxybenzaldehyde	Vanillin
6	0.700	Ethyl acetate	Ethyl butyrate
7	0.693	L-menthol	L-menthone
8	0.690	Isoamyl acetate	Isoamyl butyrate
9	0.689	(−)-limonene	(−)-terpinen-4-ol
10	0.688	Benzaldehyde	*o*-anisaldehyde
11	0.687	4-hydroxybenzaldehyde	Guaiacol
12	0.665	Methyl valerate	Pentanal
13	0.662	D-camphor	Naphthalene
14	0.660	Vanillin	Guaiacol
15	0.660	Isoamyl acetate	α-phellandrene
16	0.659	*p*-anisaldehyde	*m*-anisaldehyde
17	0.652	2-hexanone	L-menthone
18	0.649	Ethyl butyrate	α-phellandrene
19	0.644	Caproic acid	Octanoic acid
20	0.639	Benzaldehyde	*m*-anisaldehyde
21	0.634	Ethyl butyrate	Isoamyl butyrate
22	0.630	Methyl valerate	Propanol
23	0.625	(+)-limonene	α-phellandrene
24	0.607	Pentanal	Pentanol
25	0.607	*m*-anisaldehyde	*o*-anisaldehyde

they differ in other functional groups (curved arrows in Fig. 7).

Many individual odorants were found to evoke patterns similar to those evoked by odorants of similar hydrocarbon structure, despite differences in functional groups. One example is menthol, which was found to be highly similar to menthone (Table 2), with additional similarity to menthyl acetate (Fig. 7). Other such pairs included the terpenes (−)-limonene and (−)-terpinen-4-ol, as well as (+)-limonene and α-phellandrene (Table 2). The five-carbon, straight-chained aldehyde pentanal evoked a pattern similar to those evoked by methyl valerate and pentanol (Table 2), which have similar hydrocarbon structural features (Fig. 1). Finally, the small odorant formic acid evoked a pattern most similar to those evoked by the other small odorants methanol and acetone (Fig. 7).

In addition to these correlations between patterns evoked by odorants that have straightforward similarities in chemical structure, there were other comparisons that were surprising. For example, α-phellandrene exhibited an unexpected degree of similarity with aliphatic esters, despite a marked difference in molecular structure (Fig. 7; Table 2).

Dorsal-centered maps of odorant representations

Our typical contour charts of bulbar activity patterns are rolled-out maps of the bulbar surface in which the bulb is opened dorsally, and the ventral extreme is represented along the horizontal midline. Other researchers illustrating ventrally situated glomeruli also have used this type of chart (Giannetti et al., 1992). We chose this otherwise arbitrary orientation to diminish the visual impact of missing values in the dorsal part of the bulb, where we occasionally lose tissue during sectioning of the fresh-frozen bulb. Most previous workers have preferred a different orientation for rolled-out maps of the bulbar surface wherein the bulb is opened ventrally and centered for display on its dorsal aspect (Land, 1973; Stewart et al., 1979; Jourdan et al., 1980; Schwob and Gottlieb, 1986; Royet et al., 1987). One new advantage of this dorsal-centered orientation is that the maps can be compared more easily to imaging of dorsal glomeruli (Rubin and Katz, 1999; Uchida et al., 2000; Meister and Bonhoeffer, 2001; Wachowiak and Cohen, 2001). In our ventral-centered maps, any response in these dorsal glomeruli would be split, peripheralized, and somewhat distorted.

Fortunately, underlying each of our contour charts is a data array that can be rearranged and re-plotted easily to produce a dorsal-centered map for comparison with other imaging approaches in the bulb. Figure 8A shows the activity pattern evoked by benzaldehyde by using our ventral-centered chart, whereas Figure 8B shows the same activity pattern in a dorsal-centered chart. Because benzaldehyde primarily activated the dorsal aspect of the bulb, the pattern in Figure 8B is easier to see than is the pattern in Figure 8A. Module maps in the two orientations are shown in Figure 8C,D. Outlined in Figure 8B,D–H is the largest area likely to be visualized in any dorsal imaging study of a rodent olfactory bulb (Rubin and Katz, 1999, 2001; Uchida et al., 2000; Meister and Bonhoeffer, 2001; Belluscio and Katz, 2001; Wachowiak and Cohen, 2001). Figure 8E shows a dorsal-centered chart of the activity evoked by pentanal, an odorant that has been investigated in most optical imaging studies (Rubin and Katz, 1999; Uchida et al., 2000; Meister and Bonhoeffer, 2001; Belluscio and Katz, 2001). Figure 8F–H illustrates in a dorsal-centered map the 2-DG uptake evoked by decanal, santalol, and α-phellandrene, patterns that can be compared with corresponding ventral-centered versions in Figures 2 and 4.

DISCUSSION

Involvement of odorant functional groups in odor representations

We report here a strong relationship between the activity of dorsal glomerular modules in the rat olfactory bulb and the presence of particular oxygen-containing functional groups, despite large variations in odorant hydrocarbon structure. The relationships between functional groups and the activity of these dorsal modules across such a large number of odorants support the hypothesis that functional groups are important determinants of the bulbar spatial activity pattern (Johnson et al., 2000a; Uchida et al., 2000). Thus, it appears that by mapping glomerular responses across the entire bulb, it is possible to generate specific predictions regarding the chemical structure of an odorant based on the spatial pattern of activity. We anticipate that future work not only will continue to test these predictions but also ultimately will formalize the predictions into a mechanistic model. In this model, simple modular activation such as that described here would be part of an identity code describing the presence or absence of crude molecular features such as functional groups. Detailed analyses of centroids within modules then would represent a spatial code that can add specific details such as the likely molecular length of the overall odorant molecule (Johnson and Leon, 2000b).

There are several important functional groups that are not present in our current odorant set (e.g., thiols, disulfides, halides, and amines). Our conclusions regarding the

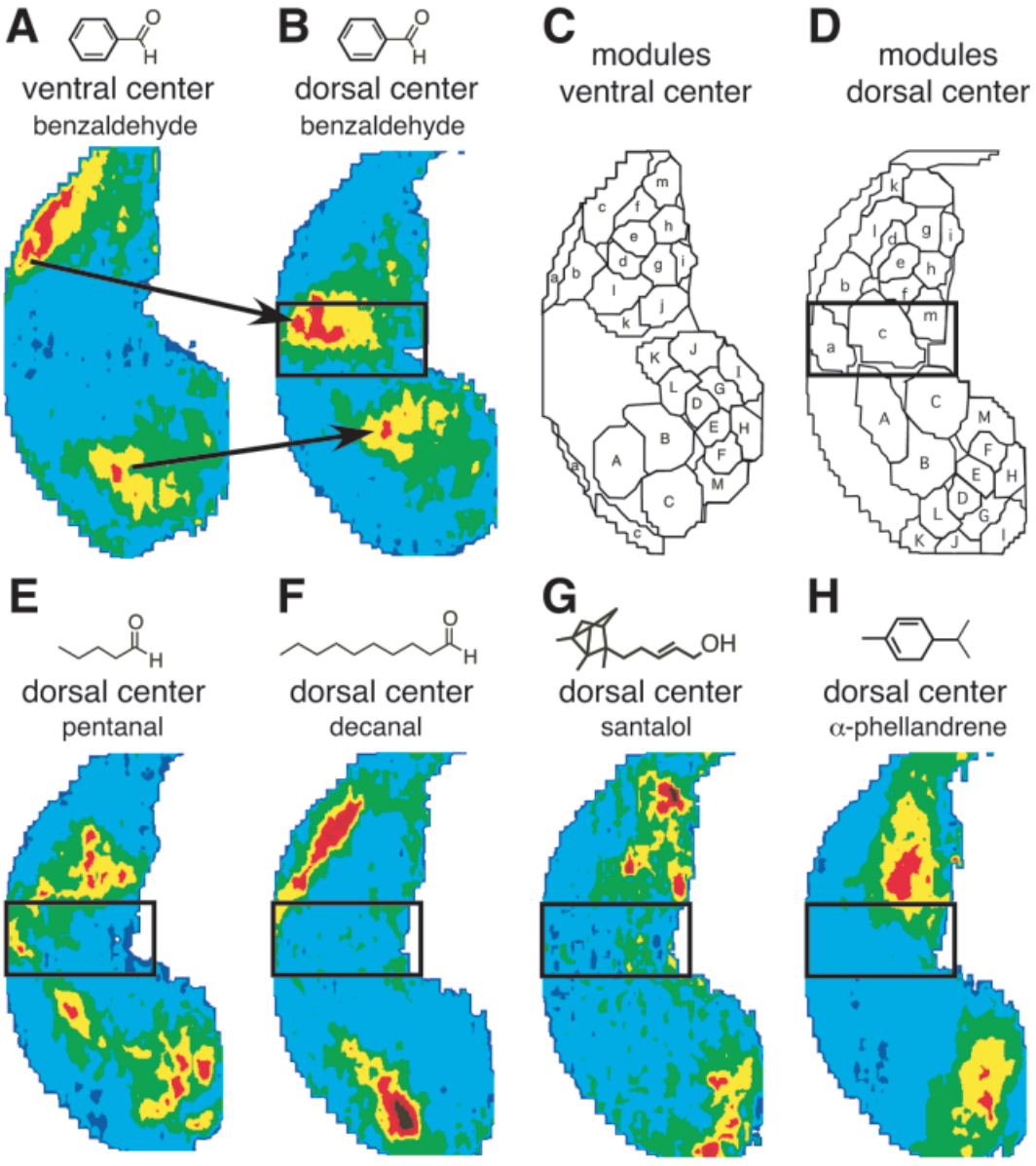

Fig. 8. Dorsal-centered renditions of contour charts. **A:** The spatial distribution of 2-deoxyglucose uptake evoked by benzaldehyde is shown by using our typical contour chart orientation, in which the ventral extreme of the bulb is oriented horizontally in the center of the chart. **B:** The array underlying the contour chart in A was transformed such that the dorsal extreme of the bulb is oriented horizontally in the center of the chart. Arrows indicate corresponding portions of the bulb in the ventral-centered and dorsal-centered contour charts. **D:** A dorsal-centered transformation of the modules chart shown in **C**. **E–H:** Odorants shown are pentanal (E), decanal (F), santalol (G), and α-phellandrene (H). Ventral-centered charts of pentanal and decanal can be found in Figure 2. Ventral-centered charts of santalol and α-phellandrene can be found in Figure 4. The rectangles in B and D–H outline approximately 15% of the glomerular layer, the largest area visualized in rodents by using optical imaging techniques that study the exposed dorsal surface of bulb. For side-by-side comparisons of dorsal- and ventral-centered contour charts showing activity evoked by each of the 54 odorants discussed in this study, please see our Web site (http://leonlab.bio.uci.edu).

relationships between a particular module or set of modules and a particular functional group may, therefore, have to be modified once additional odorants bearing these new functional groups are tested. On the other hand, it seems possible that odorants possessing these untested molecular features will activate parts of the rostral and ventral bulb that so far have been devoid of high uptake foci (Fig. 5).

Our maps consistently have shown a close relationship between the patterns of activity evoked by alcohols and aldehydes of similar hydrocarbon structure. The overall similarity between activity patterns evoked by corresponding alcohols and aldehydes suggests that the two functional groups might be recognized as similar by a large number of odorant receptors. Alternatively, there is alcohol dehydrogenase activity in the olfactory mucosa

(Thornton-Manning and Dahl, 1997), and it is, therefore, possible that alcohols are converted enzymatically to aldehydes before the activation of the olfactory receptors responsible for these activity patterns.

We also found that glomerular modules can recognize molecular features other than functional groups. Specifically, it appears that glomerular modules in the posterior, ventral part of the bulb detect odorant features involving dense hydrocarbon hydrogens and the absence of oxygen functional groups, such as were present in limonene, α-phellandrene, and β-pinene. As evidenced by responses of these glomeruli to santalol, these features can be detected even if distant parts of the same molecule do bear oxygen-containing functional groups. Perhaps the odorant receptors associated with these glomeruli rely heavily on hydrophobic interactions for the recognition of their odorant ligands. It is interesting to note that overall hydrocarbon content tends to be associated with more ventral responses in several other parts of the bulb. For example, the most intense ventral activity that we have yet observed was evoked by decanal, which has a long hydrophobic domain and which stimulated large modules ventral and caudal to modules "b" and "B" (Figs. 2, 8). More ventral activity also was correlated with greater hydrocarbon content in our prior studies of both aliphatic esters (Johnson et al., 1998) and aliphatic acids (Johnson et al., 1999). In mice, ventral glomeruli are activated differentially by urine from donors with different major histocompatibility complex genes (Schaefer et al., 2001). It will be of interest to determine whether the individual odorant features contributing to the distinctive urine odors involve particularly hydrophobic domains, as our data suggest.

Relationships between spatial activity maps and odor codes

We have begun to describe a code wherein individual chemical features of odorant molecules are transformed into neural activity within individual glomerular modules of the olfactory bulb. We have characterized the specificity of enough of these modules to predict with reasonable confidence aspects of the spatial pattern of activity given knowledge of the oxygen-containing functional groups present in an odorant. More importantly, we can begin to predict the presence of particular functional groups from the activity pattern, suggesting that odorant chemistry may indeed be encoded in the pattern.

It is important to note that we regard the dimensions of the glomerular modules as hypotheses generated from the odorant-evoked activity data that we have thus far collected. We fully expect that the borders of these modules may change somewhat as we expand the selection of odorants that we test. Indeed, new modules may even emerge if we find new specificities in the glomerular response pattern. Nevertheless, we have demonstrated how these hypotheses regarding response domains can be very accurate in predicting the kinds of molecules that will stimulate them. The nonoverlapping modules were derived operationally by identifying areas of overlap between averaged patterns evoked by different odorants. Individual odorants occasionally stimulated adjacent modules, so that these borders were not necessarily evident for each odorant or each animal. Also, individual odorants usually stimulated only a portion of each module, suggesting the possibility of "submodules" within the currently defined modules. Indeed, in individual bulbs of individual animals, glomeruli taking up 2-DG occasionally were interrupted by inactive glomeruli, as was seen in earlier studies of 2-DG uptake (Jourdan et al., 1980), as well as in studies using other imaging techniques (Meister and Bonhoeffer, 2001; Wachowiak and Cohen, 2001). Our averaging procedures obscure such details of the response within modules. In addition, because modules are identified from an average of a finite sample of animals, our ability to define boundaries also is compromised by experimental and biological variance in the locations of responses between individual animals. Issues regarding the detailed microstructure of glomerular modules perhaps would be better addressed by using other imaging techniques that allow multiple odorants to be studied in individual animals (Rubin and Katz, 1999; Uchida et al., 2000; Meister and Bonhoeffer, 2001; Wachowiak and Cohen, 2001). At the same time, given that the location of specific glomeruli is probabilistic (Strotmann et al., 2000), the concept of a response domain such as emerges from studies of 2-DG uptake seems particularly appropriate for the understanding of olfactory coding. On balance, it appears that the ability of glomerular response modules to predict response patterns from odorant chemistry is remarkably powerful, arguing that a real biological foundation underlies this hypothetical construct.

How do animals use this map of odorant chemistry in their perceptions? Despite our ability to draw parallels between odorant chemistry and activity within individual modules of the olfactory bulb, the question remains open as to how this information is involved in generating an odor perception. Any simple relationship between bulbar spatial activity patterns and odor perception would be somewhat surprising, given the further processing that must occur in olfactory cortical areas, where the tidy segregation of activity into glomerular modules is further divided into distributed patches (Haberly and Price, 1977; Zou et al., 2001). There is no evidence that animals perceive separately the individual functional groups (or other molecular features) that comprise any individual odorant. That is, although we can classify odorants as ketones or acids by looking at the spatial activity patterns, there is little evidence that the olfactory system uses this classification to generate odor perceptions. Indeed, there also is little evidence that animals can perceive separately the individual chemical components of most mixtures of different odorants (Laing and Francis, 1989; Jinks and Laing, 1999). Rather, most individual odorants and odorant mixtures appear to evoke a single, undivided odor perception.

Odorants possessing similar functional groups nevertheless do seem to share odor qualities (e.g., many esters smell fruity and many acids are pungent) (Moncrieff, 1967; Polak, 1973), and chemists can use odors to judge the presence of certain functional groups (Schafer and Brower, 1975). In addition, odorants evoking similar activity patterns apparently are perceived by rats as having similar odors, particularly if the rats have not been trained specifically to distinguish such odorants (Linster et al., 2001). For example, a similarity between spatial patterns of 2-DG uptake successfully predicted that rats initially would confuse D- and L-limonene (Linster et al., 2001), even though there is no obvious similarity between the odors of orange and turpentine reported by humans for

these two molecules. An analysis of the spatial patterns of olfactory bulb activity, therefore, clearly is relevant to predicting odor perception.

Dorsal-centered maps

Whenever three-dimensional structures are mapped onto two dimensions, there is a tendency for distortions concerning relative distances and areas of objects at different locations on the original structure. To reduce the impact of the distortions of the dorsal bulb present in our ventral-centered contour charts, we have provided here dorsal-centered renditions of some of these charts (Fig. 8). We also are making available on our Web site (http://leonlab.bio.uci.edu) dorsal-centered charts together with all of the ventral-centered charts that we have described for the odorants in the present study.

Archives and neuroinformatics of odor representations

Rats have been estimated to express approximately 1,000 distinct odorant receptor genes (Axel, 1995; Buck, 1996). Humans, who may express only several hundred receptors (Glusman et al., 2001), have been estimated to perceive hundreds of thousands of distinct odors. Obviously, this large population of both receptors and perceptions cannot be sampled effectively by using only a few dozen odorants. Therefore, we intend to continue to explore spatial activity patterns evoked by many more odorants possessing additional molecular features. As the odorant sample grows, it will become important to develop tools to access the large amount of data. Our standardized presentation of activity patterns is particularly well suited to provide this uniform access. The archive of patterns on our Web site should be useful for other researchers interested in choosing odorants that stimulate any particular area of the bulb, comparing bulbar activity patterns with different techniques, predicting likely ligands for identified receptors associated with olfactory receptor neurons, or determining the topography of connections between the bulb and other olfactory structures. In addition to this qualitative archive, data arrays such as our own also provide quantitative tools to reveal unexpected similarities or dissimilarities between particular pairs of odorant-evoked activity patterns, such as the similarity between patterns evoked by α-phellandrene and aliphatic esters discovered by way of correlation analysis. Such similarities and dissimilarities then can be used to predict differential behavior to test the relevance of these spatial patterns to olfactory perception. In addition, the modular analyses should allow us to relate activity in other bulbar regions to other interesting aspects of odorant structure.

Examining the response of the entire glomerular layer to a relatively large number of odorants with systematically different molecular features has allowed us to reveal shared responses of odorants with shared molecular features across approximately 80% of the bulb. The reliability and systematic nature of these responses also have allowed us to predict the glomerular responses of novel odorants with features similar to those that we have tested previously. The successful prediction of the identity of specific molecules from their evoked glomerular response, as well as the successful prediction of the glomerular response from specific aspects of the molecules that evoked them, suggest that we have begun to understand at least part of the olfactory code.

LITERATURE CITED

Astic L, Saucier D. 1986. Anatomical mapping of the neuroepithelial projection to the olfactory bulb in the rat. Brain Res Bull 16:445–454.

Axel R. 1995. The molecular logic of smell. Sci Am 273:154–159.

Belluscio L, Katz LC. 2001. Symmetry, stereotypy, and topography of odorant representations in mouse olfactory bulbs. J Neurosci 21:2113–2122.

Buck LB. 1996. Information coding in the vertebrate olfactory system. Annu Rev Neurosci 19:517–544.

Giannetti N, Saucier D, Astic L. 1992. Organization of the septal organ projection to the main olfactory bulb in adult and newborn rats. J Comp Neurol 323:288–298.

Glusman G, Yanai I, Rubin I, Lancet D. 2001. The complete human olfactory subgenome. Genome Res 11:685–702.

Haberly LB, Price JL. 1977. The axonal projection patterns of the mitral and tufted cells of the olfactory bulb in the rat. Brain Res 129:152–157.

Hass HB, Newton RF. 1975. Correction of boiling points to standard pressure. In: Weast RC, editor. Handbook of chemistry and physics. 56th ed. Cleveland: CRC Press. p D176–D177.

Jinks A, Laing DG. 1999. Temporal processing reveals a mechanism for limiting the capacity of humans to analyze odor mixtures. Brain Res Cogn Brain Res 8:311–325.

Johnson BA, Leon M. 2000a. Modular representations of odorants in the glomerular layer of the rat olfactory bulb and the effects of stimulus concentration. J Comp Neurol 422:496–509.

Johnson BA, Leon M. 2000b. Odorant molecular length: one aspect of the olfactory code. J Comp Neurol 426:330–338.

Johnson BA, Woo CC, Leon M. 1998. Spatial coding of odorant features in the glomerular layer of the rat olfactory bulb. J Comp Neurol 393:457–471.

Johnson BA, Woo CC, Hingco EE, Pham KL, Leon M. 1999. Multidimensional chemotopic responses to n-aliphatic acid odorants in the rat olfactory bulb. J Comp Neurol 409:529–548.

Jourdan F, Duveau A, Astic L, Holley A. 1980. Spatial distribution of [^{14}C]2-deoxyglucose uptake in the olfactory bulbs of rats stimulated with two different odours. Brain Res 188:139–154.

Laing DG, Francis GW. 1989. The capacity of humans to identify odors in mixtures. Physiol Behav 46:809–814.

Land LJ. 1973. Localized projection of olfactory nerves to rabbit olfactory bulb. Brain Res 63:153–166.

Linster C, Johnson BA, Yue E, Morse A, Xu Z, Hingco EE, Choi Y, Choi M, Messiha A, Leon M. 2001. Perceptual correlates of neural representations evoked by odorant enantiomers. J Neurosci 21:9837–9843.

Ma M, Greer CA, Shepherd GM. 2001. Functional characterization of the mouse septal organ. Soc Neurosci Abstr 27:61.14.

Malnic B, Hirono J, Sato T, Buck LB. 1999. Combinatorial receptor codes for odors. Cell 96:713–723.

Mann J, Davidson RS, Hobbs JB, Banthorpe DV, Harborne JB. 1993. Natural products: their chemistry and biological importance. Edinburgh Gate, UK: Addison Wesley Longman.

Marshall DA, Maruniak JA. 1986. Masera's organ responds to odorants. Brain Res 366:329–332.

Meister M, Bonhoeffer T. 2001. Tuning and topography in an odor map on the rat olfactory bulb. J Neurosci 21:1351–1360.

Mombaerts P, Wang F, Dulac C, Chao SK, Nemes A, Mendelsohn M, Edmonson J, Axel R. 1996. Visualizing an olfactory sensory map. Cell 87:675–686.

Moncrieff RW. 1967. The chemical senses. London: Leonard Hill.

Polak EH. 1973. Multiple profile-multiple receptor site model for vertebrate olfaction. J Theor Biol 40:469–484.

Ressler KJ, Sullivan SL, Buck LB. 1994. Information coding in the olfactory system: evidence for a stereotyped and highly organized epitope map in the olfactory bulb. Cell 79:1245–1255.

Royet JP, Sicard G, Souchier C, Jourdan F. 1987. Specificity of spatial patterns of glomerular activation in the mouse olfactory bulb: computer-assisted image analysis of 2-deoxyglucose autoradiograms. Brain Res 417:1–11.

Rubin BD, Katz LC. 1999. Optical imaging of odorant representations in the mammalian olfactory bulb. Neuron 23:499–511.

Rubin BD, Katz LC. 2001. Spatial coding of enantiomers in the rat olfactory bulb. Nat Neurosci 4:355–356.

Schaefer ML, Young DA, Restrepo D. 2001. Olfactory fingerprints for major histocompatibility complex-determined body odors. J Neurosci 21: 2481–2487.

Schafer R, Brower KR. 1975. Psychophysical recognition of functional groups on odorant molecules. In: Denton DA, Coghlan JP, editors. Olfaction and taste V. New York: Academic Press. p 313–316.

Schwob JE, Gottlieb DI. 1986. The primary olfactory projection has two chemically distinct zones. J Neurosci 6:3393–3404.

Schoenfeld TA, Clancy AN, Forbes WB, Macrides F. 1994. The spatial organization of the peripheral olfactory system of the hamster. I. Receptor neuron projections to the main olfactory bulb. Brain Res Bull 34:183–210.

Scott JW, Davis LM, Shannon D, Kaplan C. 1996. Relation of chemical structure to spatial distribution of sensory responses in rat olfactory epithelium. J Neurophysiol 75:2036–2049.

Scott JW, Shannon DE, Charpentier J, Davis LM, Kaplan C. 1997. Spatially organized response zones in rat olfactory epithelium. J Neurophysiol 77:1950–1962.

Scott JW, Brierly T, Schmidt FH. 2000. Chemical determinants of the rat electro-olfactogram. J Neurosci 20:4721–4731.

Segel IH. 1975. Biochemical calculations. New York: John Wiley and Sons.

Stewart WB, Kauer JS, Shepherd GM. 1979. Functional organization of rat olfactory bulb analysed by the 2-deoxyglucose method. J Comp Neurol 185:715–734.

Strotmann J, Conzelmann S, Beck A, Feinstein P, Breer H, Mombaerts P. 2000. Local permutations in the glomerular array of the mouse olfactory bulb. J Neurosci 20:6927–6938.

Thornton-Manning JR, Dahl AR. 1997. Metabolic capacity of nasal tissue interspecies comparisons of xenobiotic-metabolizing enzymes. Mutat Res 380:43–59.

Uchida N, Takahashi YK, Tanifuji M, Mori K. 2000. Odor maps in the mammalian olfactory bulb: domain organization and odorant structural features. Nat Neurosci 3:1035–1043.

Vassar R, Chao SK, Sitcheran R, Nuñez JM, Vosshall LB, Axel R. 1994. Topographic organization of sensory projections to the olfactory bulb. Cell 79:981–991.

Wachowiak M, Cohen LB. 2001. Representation of odorants by receptor neuron input to the mouse olfactory bulb. Neuron 32:723–735.

Zou Z, Horowitz LF, Montmayeur JP, Snapper S, Buck LB. 2001. Genetic tracing reveals a stereotyped sensory map in the olfactory cortex. Nature 414:173–179.